A&A 591, A62 (2016)
DOI: 10.1051/0004-6361/201628526

Astronomy & Astrophysics

The *Gaia*-ESO Survey: Inhibited extra mixing in two giants of the open cluster Trumpler 20?⋆

R. Smiljanic[1], E. Franciosini[2], S. Randich[2], L. Magrini[2], A. Bragaglia[3], L. Pasquini[4], A. Vallenari[5], G. Tautvaišienė[6], K. Biazzo[7], A. Frasca[7], P. Donati[3,8], E. Delgado Mena[9], A. R. Casey[10], D. Geisler[11], S. Villanova[11], B. Tang[11], S. G. Sousa[9], G. Gilmore[10], T. Bensby[12], P. François[13,14], S. E. Koposov[10], A. C. Lanzafame[15], E. Pancino[2,16], A. Recio-Blanco[17], M. T. Costado[18], A. Hourihane[10], C. Lardo[19], P. de Laverny[17], J. Lewis[10], L. Monaco[20], L. Morbidelli[2], G. G. Sacco[2], C. C. Worley[10], S. Zaggia[5], and S. Martell[21]

[1] Department for Astrophysics, Nicolaus Copernicus Astronomical Center, ul. Rabiańska 8, 87-100 Toruń, Poland
e-mail: rsmiljanic@camk.edu.pl
[2] INAF–Osservatorio Astrofisico di Arcetri, Largo Enrico Fermi 5, 50125 Firenze, Italy
[3] INAF–Osservatorio Astronomico di Bologna, via Ranzani 1, 40127 Bologna, Italy
[4] European Southern Observatory, Karl-Schwarzschild-Str. 2, 85748 Garching bei München, Germany
[5] INAF–Osservatorio Astronomico di Padova, Vicolo Osservatorio 2, 35122 Padova, Italy
[6] Institute of Theoretical Physics and Astronomy, Vilnius University, Goštauto 12, 01108 Vilnius, Lithuania
[7] INAF–Osservatorio Astrofisico di Catania, via S. Sofia 78, 95123 Catania, Italy
[8] Dipartimento di Astronomia, Università di Bologna, via Ranzani 1, 40127 Bologna, Italy
[9] Instituto de Astrofísica e Ciências do Espaço, Universidade do Porto, Rua das Estrelas, 4150-762 Porto, Portugal
[10] Institute of Astronomy, University of Cambridge, Madingley Road, Cambridge CB3 0HA, UK
[11] Departamento de Astronomía, Universidad de Concepción, Casilla 160-C, Concepción, Chile
[12] Lund Observatory, Department of Astronomy and Theoretical Physics, Box 43, 221 00 Lund, Sweden
[13] GEPI, Observatoire de Paris, PSL Research University, CNRS, Univ. Paris Diderot, Sorbonne Paris Cité, 61 avenue de l'Observatoire, 75014 Paris, France
[14] Université de Picardie Jules Verne, Physics Dpt., 33 rue St Leu, 80000 Amiens, France
[15] Dipartimento di Fisica e Astronomia, Sezione Astrofisica, Universitá di Catania, via S. Sofia 78, 95123 Catania, Italy
[16] ASI Science Data Center, via del Politecnico SNC, 00133 Roma, Italy
[17] Laboratoire Lagrange, Université Côte d'Azur, Observatoire de la Côte d'Azur, CNRS, Bd de l'Observatoire, CS 34229, 06304 Nice Cedex 4, France
[18] Instituto de Astrofísica de Andalucía-CSIC, Apdo. 3004, 18080 Granada, Spain
[19] Astrophysics Research Institute, Liverpool John Moores University, 146 Brownlow Hill, Liverpool L3 5RF, UK
[20] Departamento de Ciencias Fisicas, Universidad Andres Bello, Republica 220, Santiago, Chile
[21] School of Physics, University of New South Wales, Sydney NSW 2052, Australia

Received 16 March 2016 / Accepted 29 April 2016

ABSTRACT

Aims. We report the discovery of two Li-rich giants, with A(Li) ~ 1.50, in an analysis of a sample of 40 giants of the open cluster Trumpler 20 (with turnoff mass ~1.8 $M_{\odot}$). The cluster was observed in the context of the *Gaia*-ESO Survey.
Methods. The atmospheric parameters and Li abundances were derived using high-resolution UVES spectra. The Li abundances were corrected for nonlocal thermodynamical equilibrium (non-LTE) effects.
Results. Only upper limits of the Li abundance could be determined for the majority of the sample. Two giants with detected Li turned out to be Li rich: star MG 340 has $A(\mathrm{Li})_{\mathrm{non-LTE}} = 1.54 \pm 0.21$ dex and star MG 591 has $A(\mathrm{Li})_{\mathrm{non-LTE}} = 1.60 \pm 0.21$ dex. Star MG 340 is on average ~0.30 dex more rich in Li than stars of similar temperature, while for star MG 591 this difference is on average ~0.80 dex. Carbon and nitrogen abundances indicate that all stars in the sample have completed the first dredge-up.
Conclusions. The Li abundances in this unique sample of 40 giants in one open cluster clearly show that extra mixing is the norm in this mass range. Giants with Li abundances in agreement with the predictions of standard models are the exception. To explain the two Li-rich giants, we suggest that all events of extra mixing have been inhibited. This includes rotation-induced mixing during the main sequence and the extra mixing at the red giant branch luminosity bump. Such inhibition has been suggested in the literature to occur because of fossil magnetic fields in red giants that are descendants of main-sequence Ap-type stars.

Key words. stars: abundances – stars: evolution – stars: late-type – open clusters and associations: individual: Trumpler 20

1. Introduction

Although not well understood, the phenomenon of Li-rich giants seems to be ubiquitous as they have been observed in different environments: open clusters, globular clusters, metal-rich

⋆ Based on observations collected at the European Organisation for Astronomical Research in the Southern Hemisphere under ESO programme 188.B-3002 (The *Gaia*-ESO Public Spectroscopic Survey).

and metal-poor field stars, the Galactic bulge, and also in dwarf galaxies (see, e.g., Hill & Pasquini 1999; Gonzalez et al. 2009; Kumar et al. 2011; Ruchti et al. 2011; Kirby et al. 2012, 2016; D'Orazi et al. 2015, and references therein).

Lithium-rich giants are usually defined as those that, after the first dredge-up, have $A(\mathrm{Li}) \geq 1.50$ dex. This limit is the post-dredge-up Li abundance of a low-mass star according to standard evolutionary models, i.e., those models that include only convection as a mixing mechanism. The first Li-rich giant was a fortuitous discovery by Wallerstein & Sneden (1982). Subsequent searches have shown that these stars comprise about 1–2% of red giants (Brown et al. 1989; Pilachowski et al. 2000). Charbonnel & Balachandran (2000) suggested that these objects appear at the luminosity bump of the red giant branch (RGB) or at the early-asymptotic giant branch (AGB) for low- and intermediate-mass stars, respectively. Other recent results preferably classify these objects as core helium-burning giants (Kumar et al. 2011; Monaco et al. 2014; Silva Aguirre et al. 2014). Nevertheless, some Li-rich giants have been found throughout the RGB (see, e.g., Alcalá et al. 2011; Monaco et al. 2011; Martell & Shetrone 2013).

Lithium-rich giants have other noteworthy characteristics that add complexity to the puzzle. Some present a far-infrared excess, suggesting a connection with enhanced mass loss (de la Reza et al. 1996). This mass-loss event can also explain the observation of complex organic and inorganic compounds detected in the infrared spectra of some Li-rich giants (de la Reza et al. 2015). In a few cases, the presence of circumstellar material has been confirmed by polarimetry (Pereyra et al. 2006). Nevertheless, not all Li-rich giants have an infrared excess (see, e.g., Jasniewicz et al. 1999; Bharat Kumar et al. 2015; Rebull et al. 2015).

Fekel & Balachandran (1993) proposed a connection between Li enrichment, fast rotation, and chromospheric activity. Lithium-rich giants seem to be more common among fast rotating stars (~50%; see, e.g., Drake et al. 2002). A strong magnetic field was detected in one Li-rich giant by Lèbre et al. (2009). Further examples of Li-rich, fast-rotating, active giants exist (e.g., Reddy et al. 2002; Kriskovics et al. 2014; Strassmeier et al. 2015).

In addition, a few Li-rich giants hosting planets have been found (e.g., Adamów et al. 2012, 2014). As proposed by Siess & Livio (1999), surface Li enrichment could be caused by planet engulfment, which also causes spin-up, magnetic field generation, and shell ejection. However, planet accretion would create a ^{9}Be enhancement that has never been detected in Li-enriched objects (de Medeiros et al. 1997; Castilho et al. 1999; Melo et al. 2005; Pasquini et al. 2014) with the exception of one F-type dwarf in the open cluster NGC 6633 (Ashwell et al. 2005). Alternatively, planet engulfment could activate internal Li production and induce its mixing to the surface (Denissenkov & Weiss 2000).

Indeed, the properties of many Li-rich giants discovered within the *Gaia*-ESO Survey (Gilmore et al. 2012; Randich & Gilmore 2013) seem to be consistent with those of giants that engulfed close-in giant planets before evolving up the RGB (Casey et al. 2016). However, a small fraction of cases still require alternative explanations. Here, we report the discovery of two Li-rich giants that could be examples of such an alternative formation channel in the open cluster Trumpler 20, which is a system of ~1.66 Gyr in age and [Fe/H] = +0.17 (Donati et al. 2014).

This paper is organized as follows. In Sect. 2 we briefly describe the data used here, the analysis, and the properties of our sample. In Sect. 3 we discuss how extra mixing is needed to explain the surface Li abundances of the majority of the sample. In Sect. 4 we discuss the two Li-rich giants and the possibility that they have avoided extra-mixing mechanisms. Finally, Sect. 5 summarizes our findings and suggests new observations that could support our interpretation of the Li enrichment in these two giants.

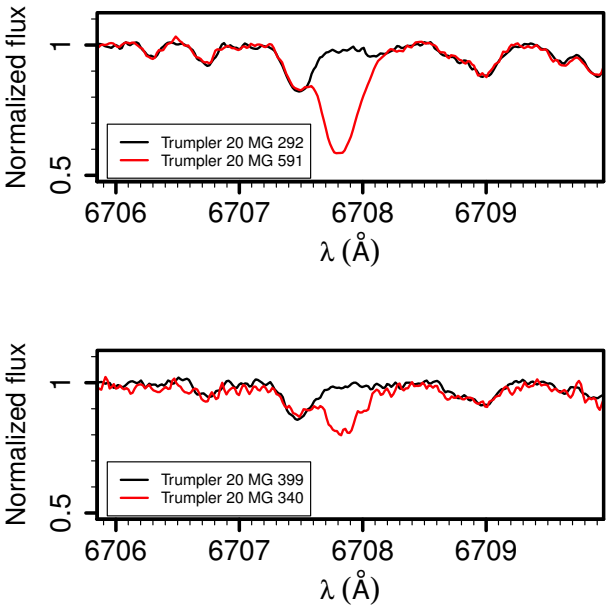

Fig. 1. Comparison of the spectra around the Li 6708 Å line between the Li-rich giants and giants with similar atmospheric parameters.

2. Data, analysis, and sample properties

The high-resolution ($R \sim 47\,000$) UVES (Ultraviolet and Visual Echelle Spectrograph, Dekker et al. 2000) spectra of 42 targets in Trumpler 20 were obtained in the context of the *Gaia*-ESO Survey. Data reduction is described in Sacco et al. (2014). Basic information on the observed giants is available in Table A.1.

The atmospheric parameters and abundances (see Table A.2) are part of the fourth *Gaia*-ESO internal data release (iDR4). The spectra were analyzed using the *Gaia*-ESO multiple pipelines strategy (Smiljanic et al. 2014) with an updated methodology (Casey et al., in prep.).

Membership was assigned using the radial velocities (RVs) as in Donati et al. (2014). Likely members (40 giants in total) are those with RV within three standard deviations of the cluster average ($\overline{\mathrm{RV}} \pm \sigma = -40.2 \pm 1.3$ km s^{-1}). One star is a subgiant[1] and one a probable nonmember (or binary) with deviant RV[2].

The Li abundances were determined from the 6708 Å line. In Fig. 1, we compare the Li 6708 Å lines of the two Li-rich giants to those of stars with similar atmospheric parameters to illustrate the Li enhancement. Corrections for nonlocal thermodynamical equilibrium (non-LTE) effects were applied using the grid of Lind et al. (2009). For the giants, the corrections range from 0.14 dex to 0.32 dex, depending on the atmospheric parameters.

The color magnitude diagram (CMD) of Trumpler 20 is shown in Fig. 2. The photometry is originally from Carraro et al. (2010) corrected for differential reddening by Donati et al. (2014). The uncertainties in the magnitudes are

[1] Trumpler 20 MG 430. The numbering system we adopt is that defined in McSwain & Gies (2005).
[2] Trumpler 20 MG 894 with RV = −35.3 km s^{-1}.

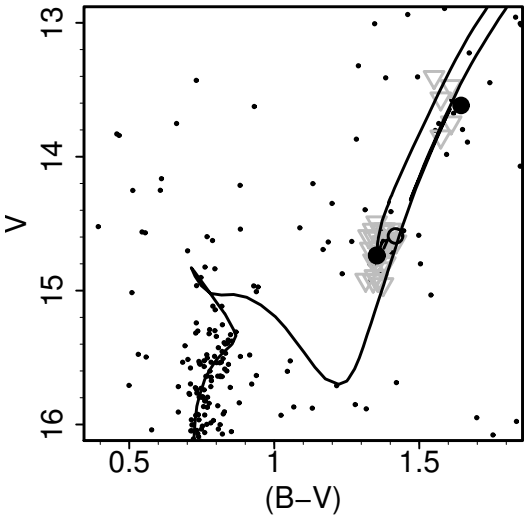

Fig. 2. Color magnitude diagram of Trumpler 20. Only stars within 3′ of the cluster center are shown. The two Li-rich giants are shown as filled circles, other giants with Li detections as open circles, giants with Li upper limits as gray triangles, and the remaining stars in the field as dots. The solid line is an isochrone from Bressan et al. (2012) with age = 1.66 Gyr and [Fe/H] = +0.17, which is the best fit to the photometric data as determined by Donati et al. (2014).

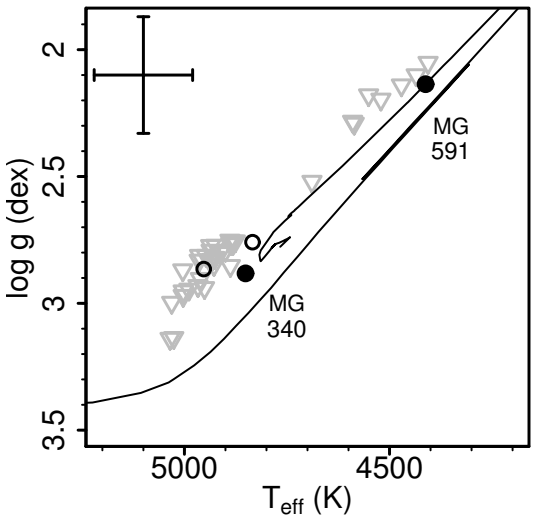

Fig. 3. Trumpler 20 giants in the $T_{\rm eff}$–log g plane. The two Li-rich giants are shown as filled circles, other giants with Li detections as open circles, and giants with Li upper limits as gray triangles. The solid line is an isochrone from Bressan et al. (2012) of 1.66 Gyr in age and [Fe/H] = +0.17, which is the best fit to the photometric data (by Donati et al. 2014). A typical error bar (±120 K and ±0.23 dex for $T_{\rm eff}$ and log g, respectively) is shown in the top left.

~0.02−0.05 mag. A noticeable feature in this CMD is the extended clump region of the cluster. Trumpler 20 is well known for its peculiar extended clump region (see Carraro et al. 2010; Platais et al. 2012; Donati et al. 2014). This feature is probably caused by the presence of two distinct clumps; the fainter clump comprises stars massive enough to start core He-burning in nondegenerate conditions and the brighter clump comprises stars with slightly lower mass that have been through the He-core flash (see, e.g., Girardi 1999; Girardi et al. 2000).

Figure 3 shows the sample in the $T_{\rm eff}$–log g plane. The group of giants with lower log g are either at the luminosity bump of the RGB or at the early-AGB, as both stages are within the error bars of the parameters in Fig. 3 and are hard to separate in the CMD of Fig. 2. We can be more confident about the evolutionary state of the group of giants with higher log g because of their chemical abundances.

The evolutionary stage of the stars is an important source of information to interpret their Li abundances, as a high Li abundance could just be indicating that the giant is actually at the bottom of the RGB (e.g., Böcek Topcu et al. 2015). Nevertheless, the C and N abundances of the giants demonstrate that they have all completed the standard first dredge-up. As shown in Fig. 4, according to the models of Lagarde et al. (2012), giants of 1.5 and 2.0 $M_{\odot}$ after the dredge-up have $C/N \sim 1$, as do all the giants in our sample. Giants at the bottom of the RGB with $T_{\rm eff} \sim 5000$ K would be in the stage before the end of the first dredge-up and thus would instead have $C/N > 3$. We can thus safely conclude that i) all the giants with $T_{\rm eff} \sim 5000$ K are in the red clump and not on the RGB and ii) that all the brightest and coolest giants have completed the Li dilution expected during the first dredge-up. The C and N abundances of the Trumpler 20 giants were discussed in Tautvaišienė et al. (2015).

3. Extra mixing in the majority of the giants

Lithium abundances have been extensively used as a tracer of mixing processes, as Li is rapidly destroyed in (p, α) reactions at

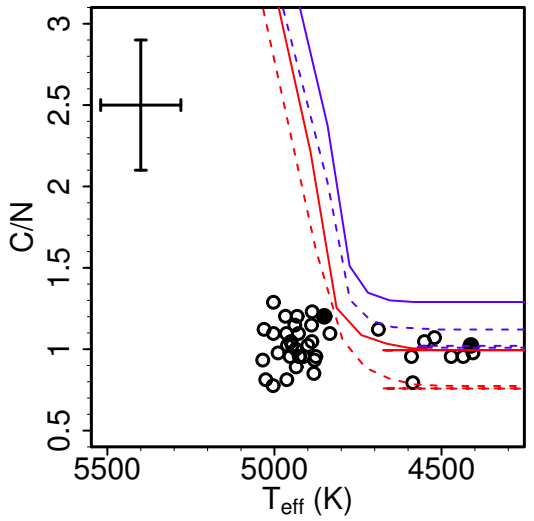

Fig. 4. C/N ratio as a function of $T_{\rm eff}$. Solid lines are the predictions of standard models and dashed lines of models with rotation-induced mixing and thermohaline mixing (Lagarde et al. 2012). Lines in blue and red are for solar metallicity stars of 1.5 $M_{\odot}$ and 2.0 $M_{\odot}$, respectively. The two Li-rich giants are shown as full circles.

temperatures above 2.5×10^6 K (Greenstein & Richardson 1951). Thus, Li only survives in the outermost layers of a star. As stars evolve to the RGB, the convective envelope deepens and Li from the surface is diluted.

Figure 5 shows the Li abundances as a function of the effective temperatures ($T_{\rm eff}$), for all cluster members, in comparison with the models of Lagarde et al. (2012). The bulk of the stars fall in between the standard and extra-mixing models (solid and dashed lines, respectively). However, care is needed in interpreting the plot because of the evolutionary state of the stars.

The solid and dashed lines in Fig. 5 are predictions for first ascent RGB stars and not for clump giants. As we showed above, our giants with $T_{\rm eff} \sim 5000$ K are clump giants and not first ascent RGB stars. The observations should not be compared to

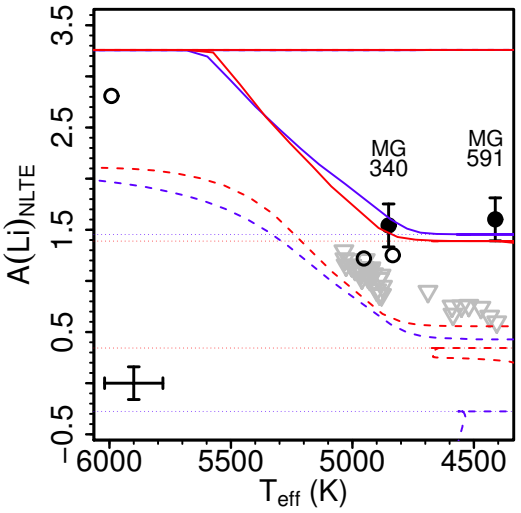

Fig. 5. Lithium abundance as a function of $T_{\rm eff}$. The two Li-rich giants are shown as filled circles, other giants with Li detections as open circles, and giants with Li upper limits as gray triangles. Solid lines are the predictions of standard models and dashed lines of models with rotation-induced mixing and thermohaline mixing (Lagarde et al. 2012). Lines in blue and red are for solar metallicity stars of 1.5 $M_{\odot}$ and 2.0 $M_{\odot}$, respectively. The dotted lines are included as an eye guide to the Li abundance level of clump giants in the models (but we note here that the clump phase does not span the $T_{\rm eff}$ range of the dotted lines in the plot).

this region of the models, but rather to the A(Li) level of core-He burning giants (the dotted lines). The clump giants have Li upper limits on average of about 0.3 dex below the two top dotted lines (standard models). For lower temperatures, the second group of stars has also Li upper limits well below the prediction of the standard models.

The clear exceptions to that are the two Li-rich giants, Trumpler 20 MG 340 and 591. This agrees with the findings of Brown et al. (1989) that giants with A(Li) $\sim$ 1.50 in agreement with standard models are a minority. Here, we are able to confirm this result in a large sample of giants of the same age, same initial chemical composition, and very similar masses. The enhanced Li depletion/dilution seen in the majority of the giants of Trumpler 20 is well documented in the literature (e.g., Lèbre et al. 1999; Pasquini et al. 2001, 2004), although the mechanism behind this extra mixing is still under debate.

We note another possible outlier, star MG 505, with $A(\mathrm{Li})_{\rm non-LTE} = 1.25 \pm 0.21$. However, because within the errors its abundance agrees with the highest upper limit at its temperature, we do not consider it among those that agree with the standard models.

4. Inhibited extra mixing in two giants

Star MG 340 has $A(\mathrm{Li})_{\rm non-LTE} = 1.54 \pm 0.21$ and $T_{\rm eff} = 4851$ K, while in eight other stars with $T_{\rm eff} = 4850 \pm 50$ K there is one detection at $A(\mathrm{Li})_{\rm non-LTE} = 1.25$ and seven upper limits below $A(\mathrm{Li})_{\rm non-LTE} \sim 1.05$. Star MG 591 has $A(\mathrm{Li})_{\rm non-LTE} = 1.60 \pm 0.21$ and $T_{\rm eff} = 4412$ K, while seven other stars with $T_{\rm eff} < 4600$ K have upper limits below $A(\mathrm{Li})_{\rm non-LTE} \sim 0.76$.

These two Li-rich giants do not show any additional chemical peculiarity when compared to the other cluster giants. Both stars seem to be single, but we do not have multiple epoch spectra to exclude long period companions. All sample giants seem to be slow rotators: $v \sin i < 4.0$ km s^{-1}. Therefore, the Li enhancement is probably not connected to rotation in the sense seen by Lèbre et al. (2006) and Carlberg et al. (2012). These authors found that in a given sample of giants, those with higher Li abundance tend to be those giants that are rotating faster, however, our giants might seem to be slow rotators because of an unfavorable line of sight. Slow rotation also argues against, but does not fully exclude, planet accretion with transfer of angular momentum as the source of the Li enhancement (see also Carlberg et al. 2016; Delgado Mena et al. 2016). Thus, external pollution as advocated by Casey et al. (2016) to explain other Li-rich giants discovered within the *Gaia*-ESO Survey seems unlikely in our case.

Internal Li production was also suggested to explain Li-rich giants. Fresh Li production might occur in the stellar interior through the ^{7}Be mechanism (Cameron & Fowler 1971). However, it is still unknown which transport mechanism would bring ^{7}Be, which decays to ^{7}Li, to the surface (Sackmann & Boothroyd 1999; Palacios et al. 2001). Charbonnel & Balachandran (2000) argued that Li-rich giants were preferentially found at the bump and the early-AGB, and connected the Li enrichment with an extra-mixing process that activates at these evolutionary stages. For low-mass stars at the bump, the extra mixing would be connected to the H-burning shell that is moving outward and removes the molecular weight discontinuity left by the receding convective layer. In intermediate-mass stars, the extra mixing would take place at the early-AGB when the convective envelope deepens again.

The two Li-rich clump giants found by Silva Aguirre et al. (2014), with A(Li) = 2.71, and Monaco et al. (2014), with A(Li) = 3.75, showed that the above scenario is at least incomplete. For clump giants, the Li enrichment could be connected to the He flash, following an episode of H injection in deeper high temperature regions (Mocák et al. 2011).

Because of the large surface convective layers of giants, the observed Li surface enrichment is likely to be short lived. A Li-rich low-mass giant that appears at the bump should not remain Li rich during its evolution to the clump. More likely, the two Li-rich giants discovered here have been freshly created during or close to their current evolutionary stages. Thus, to explain our Li-rich giants with internal Li production would require a combination of the two distinct scenarios above. One Li-rich giant would be created by mixing induced by the He flash, the other would be created by extra mixing at the bump. It also seems an odd coincidence that we would happen to observe both Li-rich giants at the moment in which their Li abundances are very close to the value expected by standard models.

While internal Li production could indeed be required to explain abundances above the meteoritic value (A(Li) > 3.0), this is perhaps not necessary to explain stars MG 340 and 591. We instead suggest that their higher Li abundance is the result of the inhibition of extra-mixing processes. Without extra mixing, their surface Li abundance is at the level predicted by standard models. In addition, this single scenario would be able to explain both giants regardless of their different evolutionary states.

If this suggestion is correct, two instances of extra mixing must have been affected. The first is the extra Li dilution beyond the predicted first dredge-up dilution, which is observed as the star leaves the main sequence toward the RGB. Observationally, it is well known that an extra mixing causes the Li dilution to start earlier than predicted by standard models (e.g., Lèbre et al. 1999; Pasquini et al. 2001, 2004). This is because rotation-induced mixing creates a Li-free region inside real stars that is larger than predicted by these models (Palacios et al. 2003). In the two Li-rich giants, rotation-induced mixing must have been

weak and the Li dilution proceeded as expected by standard models.

The second extra-mixing event to be avoided is the event taking place at the luminosity bump of the RGB (see Lagarde et al. 2012, and references therein). The luminosity bump (see, e.g., Christensen-Dalsgaard 2015) happens at the RGB of low-mass stars when the hydrogen-burning shell reaches the composition discontinuity left behind by the first dredge-up. The current best candidate for the mechanism behind this extra mixing seems to be thermohaline mixing (Charbonnel & Zahn 2007b), although there are discussions about the physical properties and efficiency of this mechanism (e.g., Maeder et al. 2013; Garaud & Brummell 2015; Lattanzio et al. 2015, and references therein).

Star MG 340 in the extended clump of the cluster is likely to be a low-mass star. As discussed by Girardi (1999), in such an extended clump, the less massive stars are actually the brighter stars. Both the CMD in Fig. 2 and the $T_{\rm eff}$–log g diagram in Fig. 3 seem to indicate that MG 340 belongs to the group of brighter giants. Thus, in our scenario, for it to keep an unaltered Li surface abundance, thermohaline mixing must have been inhibited. On the other hand, star MG 591 is either on the bump or on the early-AGB. If on the early-AGB, then it is an intermediate-mass star that does not go through both the He-flash and the bump phase. However, it would still need to inhibit thermohaline mixing at the early-AGB (see Lagarde et al. 2012, and references therein). If on the bump, it either avoided thermohaline mixing or did not activate it yet. All other giants with similar $T_{\rm eff}$ and log g have lower Li abundances. This could indicate that star MG 591 is also after the moment where thermohaline mixing becomes efficient. As pointed out by the referee, however, at this phase stars ascend and reascend the RGB, crossing the same $T_{\rm eff}$ and log g region three times. Therefore, it is plausible that at least one star among the group at the bump has not yet activated thermohaline mixing. If this is the case, star MG 591 would not be an Li-rich giant, but a normal giant in a stage before extra mixing was activated.

Extra-mixing inhibition is not a new idea. Based on carbon isotopic ratios, ^{12}C/^{13}C, Charbonnel & Do Nascimento (1998) estimated that about 4% of low-mass giants do not experience extra mixing on the RGB. Charbonnel & Zahn (2007a) suggested that extra mixing is avoided by giants that are descendant from Ap-type main-sequence stars. In these stars, fossil magnetic fields would be able to inhibit thermohaline mixing. Modern estimates of the percentage of Ap stars with respect to nonmagnetic A-type stars are between 1.7−3.5% (North 1993; Power et al. 2007). This is consistent with finding one or two stars in our sample of 40 giants of Trumpler 20 (a fraction of 2.5 or 5%). In addition, the stellar mass of our giants is within the mass range of Ap stars (∼1.5 to 3.6 $M_{\odot}$, Power et al. 2007).

5. Summary

In this work, we presented the discovery of two Li-rich giants in the open cluster Trumpler 20. These two stars were identified in an analysis of a sample of 40 giants for which high-resolution spectra were obtained with UVES in the context of the *Gaia*-ESO public spectroscopic survey. This provides a unique large sample of giants that have the same age, same initial chemical composition, and very similar masses. The Li abundances in this sample clearly demonstrate that extra mixing is the norm in stars in this mass range. Giants with Li abundances in agreement with the predictions of standard models are the exception.

To explain the two Li-rich giants, we suggest that all instances of extra-mixing processes have been inhibited. Because of that, the surface Li abundance in these two stars remained at the level predicted by standard stellar evolution models, i.e., A(Li) ∼ 1.50. We argue that the fraction of Li-rich giants found in our sample is consistent with these giants being evolved counterparts of magnetic Ap-type dwarfs. In this case, the extra-mixing processes could have been inhibited by the action of magnetic fields, as suggested by Charbonnel & Zahn (2007a).

Other explanations seem less likely, although they cannot be fully excluded. Extra Li from the accretion of external material should be accompanied by accretion of angular momentum, but there is no evidence of fast rotation in the two giants. Because the two Li-rich giants have different evolutionary stages, internal Li production would require two different mechanisms to bring the fresh Li to the surface. The extra-mixing inhibition hypothesis would instead be able to explain both giants at the same time.

Additional observations could help in providing extra support to our suggested scenario, or they could help to disprove it. First, if no extra mixing took place, the carbon isotopic ratio should be close to the prediction of standard models, ^{12}C/^{13}C ∼ 30. We could not determine the carbon isotopic ratio because the region around 8000 Å, containing the CN bands preferred for this type of analysis in metal-rich giants, is not part of the *Gaia*-ESO spectra.

Second, there should likely be signs of magnetic activity in the Li-rich giants. Other candidates of Ap-type stars descendants were identified among giants and subgiants with magnetic activity (e.g., Aurière et al. 2014). However, fossil magnetic fields beneath the surface are hard to detect (Aurière et al. 2015; Stello et al. 2016). Nevertheless, the core-He burning star MG 340 is at one of the evolutionary phases where magnetic activity in giants is observed (Aurière et al. 2015). We checked the Hα line in our spectrum, but it shows no evident sign of activity. This is not inconsistent, as not all active giants display emission in Hα (see, e.g., Fekel & Balachandran 1993). Emission should be clearer in the Ca H and K lines or in the UV, which are not part of our spectra.

Finally, if such a scenario of extra-mixing inhibition is correct, it would likely apply to many, if not all, Li-rich giants with A(Li) ∼ 1.50 (or slightly higher) and masses between ∼1.5 and 3.6 $M_{\odot}$. They would not have experienced fresh Li production, but would instead have preserved part of their original Li abundance.

Acknowledgements. We thank the anonymous referee for his/her suggestions and very fast report. R.S. acknowledges support by the National Science Center of Poland through grant 2012/07/B/ST9/04428. S.V. gratefully acknowledges the support provided by FONDECYT reg. n. 1130721. G.T. acknowledges support by the Research Council of Lithuania (MIP-082/2015). D.G. gratefully acknowledges support from the Chilean BASAL Centro de Excelencia en Astrofísica y Tecnologías Afines (CATA) grant PFB-06/2007. S.G.S. acknowledges the support from FCT through Investigador FCT contract of reference IF/00028/2014. E.D.M. acknowledges the support from FCT in the form of the grant SFRH/BPD/76606/2011. S.G.S. and E.D.M. also acknowledge the support from FCT through the project PTDC/FIS-AST/7073/2014. Based on data products from observations made with ESO Telescopes at the La Silla Paranal Observatory under program ID 188.B-3002. These data products have been processed by the Cambridge Astronomy Survey Unit (CASU) at the Institute of Astronomy, University of Cambridge, and by the FLAMES/UVES reduction team at INAF/Osservatorio Astrofisico di Arcetri. These data have been obtained from the *Gaia*-ESO Survey Data Archive, prepared and hosted by the Wide Field Astronomy Unit, Institute for Astronomy, University of Edinburgh, which is funded by the UK Science and Technology Facilities Council. This work was partly supported by the European Union FP7 program through ERC grant number 320360 and by the Leverhulme Trust through grant RPG-2012-541. We acknowledge the support from INAF and Ministero dell' Istruzione, dell' Università' e della Ricerca (MIUR) in the form of the grant "Premiale VLT 2012" and "The Chemical and Dynamical Evolution of the Milky Way and Local Group Galaxies". The results presented here benefit from discussions held during

the *Gaia*-ESO workshops and conferences supported by the ESF (European Science Foundation) through the GREAT Research Network Programme.

References

Adamów, M., Niedzielski, A., Villaver, E., Nowak, G., & Wolszczan, A. 2012, ApJ, 754, L15
Adamów, M., Niedzielski, A., Villaver, E., Wolszczan, A., & Nowak, G. 2014, A&A, 569, A55
Alcalá, J. M., Biazzo, K., Covino, E., Frasca, A., & Bedin, L. R. 2011, A&A, 531, L12
Ashwell, J. F., Jeffries, R. D., Smalley, B., et al. 2005, MNRAS, 363, L81
Aurière, M., Lignières, F., Konstantinova-Antova, R., et al. 2014, in Putting A Stars into Context: Evolution, Environment, and Related Stars, eds. G. Mathys, E. R. Griffin, O. Kochukhov, R. Monier, & G. M. Wahlgren, 444
Aurière, M., Konstantinova-Antova, R., Charbonnel, C., et al. 2015, A&A, 574, A90
Bharat Kumar, Y., Reddy, B. E., Muthumariappan, C., & Zhao, G. 2015, A&A, 577, A10
Böcek Topcu, G., Afşar, M., Schaeuble, M., & Sneden, C. 2015, MNRAS, 446, 3562
Bressan, A., Marigo, P., Girardi, L., et al. 2012, MNRAS, 427, 127
Brown, J. A., Sneden, C., Lambert, D. L., & Dutchover, Jr., E. 1989, ApJS, 71, 293
Cameron, A. G. W., & Fowler, W. A. 1971, ApJ, 164, 111
Carlberg, J. K., Cunha, K., Smith, V. V., & Majewski, S. R. 2012, ApJ, 757, 109
Carlberg, J. K., Smith, V. V., Cunha, K., & Carpenter, K. G. 2016, ApJ, 818, 25
Carraro, G., Costa, E., & Ahumada, J. A. 2010, AJ, 140, 954
Casey, A. R., Ruchti, G., Masseron, T., et al. 2016, MNRAS, submmitted [arXiv:1603.03038]
Castilho, B. V., Spite, F., Barbuy, B., et al. 1999, A&A, 345, 249
Charbonnel, C., & Balachandran, S. C. 2000, A&A, 359, 563
Charbonnel, C., & Do Nascimento, Jr., J. D. 1998, A&A, 336, 915
Charbonnel, C., & Zahn, J.-P. 2007a, A&A, 476, L29
Charbonnel, C., & Zahn, J.-P. 2007b, A&A, 467, L15
Christensen-Dalsgaard, J. 2015, MNRAS, 453, 666
de la Reza, R., Drake, N. A., & da Silva, L. 1996, ApJ, 456, L115
de la Reza, R., Drake, N. A., Oliveira, I., & Rengaswamy, S. 2015, ApJ, 806, 86
de Medeiros, J. R., Lebre, A., de Garcia Maia, M. R., & Monier, R. 1997, A&A, 321, L37
Dekker, H., D'Odorico, S., Kaufer, A., Delabre, B., & Kotzlowski, H. 2000, in Optical and IR Telescope Instrumentation and Detectors, eds. M. Iye, & A. F. Moorwood, SPIE Conf. Ser., 4008, 534
Delgado Mena, E., Tsantaki, M., Sousa, S. G., et al. 2016, A&A, 587, A66
Denissenkov, P. A., & Weiss, A. 2000, A&A, 358, L49
Donati, P., Cantat Gaudin, T., Bragaglia, A., et al. 2014, A&A, 561, A94
D'Orazi, V., Gratton, R. G., Angelou, G. C., et al. 2015, ApJ, 801, L32
Drake, N. A., de la Reza, R., da Silva, L., & Lambert, D. L. 2002, AJ, 123, 2703
Fekel, F. C., & Balachandran, S. 1993, ApJ, 403, 708
Garaud, P., & Brummell, N. 2015, ApJ, 815, 42
Gilmore, G., Randich, S., Asplund, M., et al. 2012, The Messenger, 147, 25
Girardi, L. 1999, MNRAS, 308, 818
Girardi, L., Mermilliod, J.-C., & Carraro, G. 2000, A&A, 354, 892
Gonzalez, O. A., Zoccali, M., Monaco, L., et al. 2009, A&A, 508, 289
Greenstein, J. L., & Richardson, R. S. 1951, ApJ, 113, 536
Grevesse, N., Asplund, M., & Sauval, A. J. 2007, Space Sci. Rev., 130, 105
Hill, V., & Pasquini, L. 1999, A&A, 348, L21
Jasniewicz, G., Parthasarathy, M., de Laverny, P., & Thévenin, F. 1999, A&A, 342, 831
Kirby, E. N., Fu, X., Guhathakurta, P., & Deng, L. 2012, ApJ, 752, L16
Kirby, E. N., Guhathakurta, P., Zhang, A. J., et al. 2016, ApJ, 819, 135
Kriskovics, L., Kővári, Z., Vida, K., Granzer, T., & Oláh, K. 2014, A&A, 571, A74
Kumar, Y. B., Reddy, B. E., & Lambert, D. L. 2011, ApJ, 730, L12
Lagarde, N., Decressin, T., Charbonnel, C., et al. 2012, A&A, 543, A108
Lattanzio, J. C., Siess, L., Church, R. P., et al. 2015, MNRAS, 446, 2673
Lèbre, A., de Laverny, P., de Medeiros, J. R., Charbonnel, C., & da Silva, L. 1999, A&A, 345, 936
Lèbre, A., de Laverny, P., Do Nascimento, Jr., J. D., & de Medeiros, J. R. 2006, A&A, 450, 1173
Lèbre, A., Palacios, A., Do Nascimento, Jr., J. D., et al. 2009, A&A, 504, 1011
Lind, K., Asplund, M., & Barklem, P. S. 2009, A&A, 503, 541
Maeder, A., Meynet, G., Lagarde, N., & Charbonnel, C. 2013, A&A, 553, A1
Martell, S. L., & Shetrone, M. D. 2013, MNRAS, 430, 611
McSwain, M. V., & Gies, D. R. 2005, ApJS, 161, 118
Melo, C. H. F., de Laverny, P., Santos, N. C., et al. 2005, A&A, 439, 227
Mocák, M., Meakin, C. A., Müller, E., & Siess, L. 2011, ApJ, 743, 55
Monaco, L., Villanova, S., Moni Bidin, C., et al. 2011, A&A, 529, A90
Monaco, L., Boffin, H. M. J., Bonifacio, P., et al. 2014, A&A, 564, L6
North, P. 1993, in IAU Colloq. 138: Peculiar versus Normal Phenomena in A-type and Related Stars, eds. M. M. Dworetsky, F. Castelli, & R. Faraggiana, ASP Conf. Ser., 44, 577
Palacios, A., Charbonnel, C., & Forestini, M. 2001, A&A, 375, L9
Palacios, A., Talon, S., Charbonnel, C., & Forestini, M. 2003, A&A, 399, 603
Pasquini, L., Randich, S., & Pallavicini, R. 2001, A&A, 374, 1017
Pasquini, L., Randich, S., Zoccali, M., et al. 2004, A&A, 424, 951
Pasquini, L., Koch, A., Smiljanic, R., Bonifacio, P., & Modigliani, A. 2014, A&A, 563, A3
Pereyra, A., Castilho, B. V., & Magalhães, A. M. 2006, A&A, 449, 211
Pilachowski, C. A., Sneden, C., Kraft, R. P., Harmer, D., & Willmarth, D. 2000, AJ, 119, 2895
Platais, I., Melo, C., Quinn, S. N., et al. 2012, ApJ, 751, L8
Power, J., Wade, G. A., Hanes, D. A., Aurier, M., & Silvester, J. 2007, in Physics of Magnetic Stars, eds. I. I. Romanyuk, D. O. Kudryavtsev, O. M. Neizvestnaya, & V. M. Shapoval, 89
Randich, S., & Gilmore, G. 2013, The Messenger, 154, 47
Rebull, L. M., Carlberg, J. K., Gibbs, J. C., et al. 2015, AJ, 150, 123
Reddy, B. E., Lambert, D. L., Hrivnak, B. J., & Bakker, E. J. 2002, AJ, 123, 1993
Ruchti, G. R., Fulbright, J. P., Wyse, R. F. G., et al. 2011, ApJ, 743, 107
Sacco, G. G., Morbidelli, L., Franciosini, E., et al. 2014, A&A, 565, A113
Sackmann, I.-J., & Boothroyd, A. I. 1999, ApJ, 510, 217
Siess, L., & Livio, M. 1999, MNRAS, 308, 1133
Silva Aguirre, V., Ruchti, G. R., Hekker, S., et al. 2014, ApJ, 784, L16
Smiljanic, R., Korn, A. J., Bergemann, M., et al. 2014, A&A, 570, A122
Stello, D., Cantiello, M., Fuller, J., et al. 2016, Nature, 529, 364
Strassmeier, K. G., Carroll, T. A., Weber, M., & Granzer, T. 2015, A&A, 574, A31
Tautvaišienė, G., Drazdauskas, A., Mikolaitis, Š., et al. 2015, A&A, 573, A55
Wallerstein, G., & Sneden, C. 1982, ApJ, 255, 577

Appendix A: Additional tables

Table A.1. Observational data for the stars of Trumpler 20.

Star ID	*Gaia*-ESO ID	RA deg (J2000)	Dec deg (J2000)	V mag	$(B-V)$ mag	RV km s^{-1}	S/N
63	12385807-6030286	189.7420	−60.5079	13.60	1.59	−40.81	109
129	12400109-6031395	190.0046	−60.5276	14.72	1.42	−40.04	58
203	12393740-6032568	189.9059	−60.5491	14.89	1.35	−40.18	43
227	12394385-6033165	189.9328	−60.5546	14.61	1.34	−40.50	50
246	12394897-6033282	189.9541	−60.5578	14.55	1.34	−39.07	44
287	12394688-6033540	189.9454	−60.5650	14.80	1.35	−40.48	53
292	12390409-6034001	189.7671	−60.5667	13.41	1.55	−40.08	98
340	12391577-6034406	189.8157	−60.5779	14.74	1.35	−40.21	49
346	12394418-6034410	189.9341	−60.5781	14.71	1.37	−40.50	50
399	12395973-6035072	189.9990	−60.5853	14.55	1.40	−41.74	78
429	12400116-6035218	190.0048	−60.5894	14.54	1.37	−39.27	59
430	12395566-6035233	189.9820	−60.5898	15.25	1.00	−41.79	35
468	12400754-6035445	190.0315	−60.5957	13.47	1.61	−39.86	83
505	12392698-6036053	189.8625	−60.6015	14.59	1.42	−40.31	66
542	12391200-6036322	189.8000	−60.6089	14.69	1.33	−40.58	60
582	12391113-6036528	189.7964	−60.6146	14.92	1.36	−40.76	49
591	12400449-6036566	190.0188	−60.6157	13.62	1.64	−40.73	88
638	12395554-6037268	189.9815	−60.6241	14.64	1.39	−40.07	83
679	12402227-6037419	190.0929	−60.6283	14.74	1.42	−41.13	47
724	12390709-6038056	189.7796	−60.6349	14.92	1.31	−38.38	46
768	12394514-6038258	189.9382	−60.6405	14.80	1.38	−40.68	56
770	12392584-6038279	189.8577	−60.6411	14.93	1.34	−42.97	36
781	12394475-6038339	189.9365	−60.6427	14.62	1.40	−37.89	52
787	12395424-6038370	189.9761	−60.6436	14.61	1.39	−42.48	65
791	12394596-6038389	189.9415	−60.6441	14.54	1.38	−38.96	65
794	12391002-6038402	189.7918	−60.6445	13.57	1.57	−40.60	87
795	12394742-6038411	189.9476	−60.6447	14.72	1.36	−39.30	46
827	12395654-6039012	189.9856	−60.6503	14.78	1.38	−38.23	57
835	12393781-6039051	189.9076	−60.6514	14.49	1.35	−39.71	45
858	12394307-6039193	189.9295	−60.6554	14.63	1.42	−40.82	54
885	12395711-6039335	189.9880	−60.6593	14.64	1.37	−41.01	62
894	12393131-6039423	189.8805	−60.6617	14.77	1.34	−35.29	56
911	12400259-6039545	190.0108	−60.6651	13.74	1.61	−40.41	106
923	12394121-6040040	189.9217	−60.6678	14.84	1.37	−41.01	56
950	12392636-6040217	189.8599	−60.6727	14.74	1.35	−40.67	42
1008	12394715-6040584	189.9465	−60.6829	13.85	1.57	−39.41	78
1010	12394049-6041006	189.9188	−60.6835	14.56	1.37	−41.99	48
1044	12400278-6041192	190.0116	−60.6887	14.95	1.38	−38.75	40
1082	12390478-6041475	189.7699	−60.6965	14.59	1.32	−40.15	52
2690	12383657-6045300	189.6525	−60.7583	14.57	1.44	−41.62	27
2730	12383597-6045242	189.6498	−60.7568	14.94	1.38	−40.08	53
3470	12402478-6043103	190.1033	−60.7195	13.92	1.60	−39.84	57

Notes. The star ID is taken from McSwain & Gies (2005). The V magnitude and $(B-V)$ color have been corrected from differential reddening by Donati et al. (2014). The radial velocities and signal-to-noise values were determined from the bluer part of the UVES spectrum as described in Sacco et al. (2014).

Table A.2. Atmospheric parameters and lithium abundances for the stars of Trumpler 20.

Star ID	$T_{\rm eff}$ (K)	σ (K)	log g (dex)	σ (dex)	[Fe/H] (dex)	σ (dex)	ξ km s^{-1}	σ km s^{-1}	A(Li)$_{\rm LTE}$ (dex)	σ (dex)	Flag	A(Li)$_{\rm non-LTE}$
63	4551	133	2.18	0.29	0.09	0.11	1.45	0.06	0.50	0.38	lim.	0.75
129	4888	116	2.85	0.23	0.13	0.10	1.39	0.04	0.85	0.05	lim.	1.02
203	5031	120	3.00	0.22	0.14	0.10	1.40	0.10	1.07	0.14	lim.	1.22
227	5004	113	2.87	0.23	0.09	0.10	1.59	0.06	1.04	0.18	lim.	1.20
246	4947	114	2.81	0.22	0.10	0.09	1.50	0.09	1.03	0.18	lim.	1.21
287	4961	116	2.90	0.23	0.14	0.09	1.38	0.06	0.87	0.12	lim.	1.03
292	4406	114	2.05	0.24	0.00	0.10	1.55	0.09	0.28	0.34	lim.	0.60
340	4851	118	2.88	0.23	0.02	0.10	1.36	0.06	1.37	0.21	det.	1.54
346	4963	118	2.81	0.23	0.15	0.10	1.47	0.13	0.92	0.14	lim.	1.08
399	4876	113	2.76	0.22	0.10	0.10	1.41	0.06	0.77	0.22	lim.	0.95
429	4887	122	2.77	0.22	0.10	0.10	1.38	0.05	0.70	0.10	lim.	0.87
430	5992	125	3.79	0.25	0.20	0.10	1.64	0.21	2.83	0.21	det.	2.81
468	4435	115	2.10	0.23	0.06	0.10	1.52	0.05	0.34	0.31	lim.	0.65
505	4834	120	2.76	0.25	0.11	0.10	1.39	0.10	1.07	0.21	det.	1.25
542	4939	112	2.83	0.23	0.15	0.10	1.33	0.05	0.93	0.20	lim.	1.09
582	4967	115	2.93	0.23	0.18	0.10	1.39	0.11	0.97	0.15	lim.	1.13
591	4412	132	2.14	0.25	0.00	0.10	1.59	0.23	1.32	0.21	det.	1.60
638	4900	112	2.79	0.22	0.13	0.10	1.38	0.05	0.74	0.20	lim.	0.91
679	4936	121	2.77	0.23	0.12	0.10	1.50	0.10	0.92	0.15	lim.	1.08
724	5026	120	3.14	0.23	0.10	0.10	1.27	0.04	1.01	0.13	lim.	1.15
768	4928	119	2.85	0.23	0.12	0.10	1.36	0.05	0.85	0.15	lim.	1.01
770	5035	119	3.14	0.25	0.12	0.10	1.28	0.07	1.15	0.14	lim.	1.29
781	4882	118	2.77	0.23	0.12	0.10	1.48	0.09	0.88	0.18	lim.	1.05
787	4913	109	2.80	0.23	0.14	0.10	1.42	0.04	0.90	0.22	lim.	1.07
791	4889	122	2.75	0.24	0.10	0.11	1.42	0.06	0.70	0.13	lim.	0.87
794	4471	118	2.14	0.23	0.01	0.10	1.56	0.17	0.43	0.05	lim.	0.74
795	4924	117	2.77	0.23	0.08	0.10	1.50	0.07	0.96	0.17	lim.	1.13
827	4932	122	2.83	0.25	0.16	0.10	1.39	0.05	0.89	0.17	lim.	1.05
835	4935	128	2.79	0.22	0.12	0.11	1.44	0.14	0.87	0.11	lim.	1.03
858	4880	117	2.76	0.23	0.12	0.09	1.34	0.05	0.69	0.11	lim.	0.87
885	4964	116	2.83	0.23	0.14	0.09	1.44	0.06	0.93	0.05	lim.	1.09
894	4988	114	3.04	0.22	0.13	0.10	1.37	0.03	0.95	0.16	lim.	1.10
911	4521	115	2.20	0.22	0.03	0.09	1.47	0.15	0.50	0.39	lim.	0.76
923	4989	117	2.94	0.25	0.13	0.09	1.41	0.03	0.96	0.17	lim.	1.11
950	4953	121	2.87	0.23	0.08	0.10	1.47	0.23	1.06	0.22	det.	1.22
1008	4586	123	2.29	0.24	0.05	0.10	1.49	0.08	0.43	0.05	lim.	0.67
1010	4926	120	2.82	0.24	0.10	0.11	1.40	0.10	0.94	0.16	lim.	1.11
1044	4951	117	2.94	0.22	0.12	0.09	1.34	0.10	0.97	0.05	lim.	1.13
1082	5003	116	2.95	0.22	0.18	0.09	1.47	0.07	1.00	0.16	lim.	1.15
2690	4689	128	2.52	0.25	−0.01	0.12	1.37	0.06	0.68	0.05	lim.	0.90
2730	5003	117	2.97	0.24	0.14	0.09	1.51	0.08	0.99	0.17	lim.	1.15
3470	4590	123	2.28	0.22	0.03	0.11	1.48	0.10	0.51	0.18	lim.	0.75

Notes. The star ID is taken from McSwain & Gies (2005). For the metallicity, we adopt $A(\mathrm{Fe})_{\odot} = 7.45$ as solar reference (Grevesse et al. 2007). The flag indicates if the Li abundance is a detection or an upper limit.